CZECHOSLOVAK ACADEMY OF SCIENCES

CZECHOSLOVAK JOURNAL OF PHYSICS

REPRINT

VOLUME B 34

1984

INVESTIGATIONS OF THE START UP PHASE IN THE TM-1-MH TOKAMAK

H. Prinzler, P. Heymann

Zentralinstitut für Elektronenphysik der AdW der DDR, 1199 Berlin, DDR

J. Stöckel, J. Badalec, F. Žáček, K. Jakubka, V. Kopecký

Institute of Plasma Physics, Czechosl. Acad. Sci., Pod vodárenskou věží 4, 182 11 Praha 8, Czechoslovakia

Experimental investigations of the start up phase of the tokamak discharge are described. Measurements of plasma current and loop voltage show an avalanche phase with exponential current growth in the first 200 μs and a pinch phase in the time between 200 μs and 400 μs. The growth rate depends on the external perpendicular magnetic fields. The relation between current and electron density and in particular the role of skin effect are discussed. The measured growth rates are explained by the balance between ionization and particle losses. The derived values of electron drift velocity v_d and ionization coefficient α are compared with the results from gas discharge physics.

1. INTRODUCTION

The start up phase of a tokamak discharge has been investigated by several authors during the last decade. The papers were aimed at the process of breakdown in toroidal geometry and their time scale [1–4] and at the optimization of the start up, i.e. the minimum energy demand for the plasma formation [5–7]. The problem of intense plasma wall interaction in this time range was investigated in [8, 9]. Except for some details the following qualitative picture has been accepted. The discharge runs through different states until it reaches the stationary hot plasma. The first one is the gas breakdown with exponential current growth (avalanche phase). Above a distinct plasma current ($I_p \doteq 1$ kA for TM-1-MH) the rotational transform is established and the plasma confinement starts (pinch phase). The electron density increases further until the plasma is fully ionized.

In this time period gas discharge processes as excitation, ionization and H-atom radiation take place, therefore the bulk electron temperature remains low ($T_e < < 20$ eV). Plasma heating does not start until the plasma has been fully ionized.

This paper deals with the avalanche phase of the TM-1-MH discharge. We relate the ionization and loss processes in order to explain the time delay between the switching-in of the OH-battery and the appearance of the density measurable by the 4 mm microwave interferometer ($n \simeq 10^{-18}$ m^{-3}).

The paper is organized as follows: The experiments are described in sec. 2. There we report on basic parameters and probe measurements in the scrape off layer. In sec. 3 we give a quantitative model of the avalanche phase regarding the electrodynamical as well as the gas discharge properties. The comparison of this model with experimental results is given in sec. 4. Conclusions are given in sec. 5.

2. EXPERIMENTAL ARRANGEMENTS AND RESULTS

The Tokamak TM-1-MH has been described earlier [10]. We made the following experiments with a toroidal magnetic field $B_T = 1{\cdot}3$ T, a maximum plasma current $I_p = 16$ kA and a variation of the vertical and horizontal magnetic fields generated by separate coil systems: $B_v = \pm 2{\cdot}25 \times 10^{-3}$ T $(2{\cdot}8 \times 10^{-3}$ T/kA) and $B_h = 0 \ldots 3{\cdot}25 \times 10^{-3}$ T $(6{\cdot}5 \times 10^{-3}$ T/kA). The filling pressure was $p = 1{\cdot}3 \times 10^{-2}$ Pa without additional gas puffing, that means $n_H = 7 \times 10^{18}$ H-atoms/m^3 after dissociation. Diagnostic methods and the direction of fields and current are shown in fig. 1. Two Langmuir probes (Mo-wire $l = 5$ mm, $d = 1$ mm) are located in the limiter shadow. They can be shifted from the liner position to the edge of the limiter projection. The H_β-line radiance was measured through the collimator of the neutral beam diagnostic system at different positions Δh. The receiving system was a photomultiplier with interference filter. Relative values only were obtained. The toroidal electric field E_T, impressed to the torus by the transformer, was determined by a measuring loop located close to the outer surface of the copper shell.

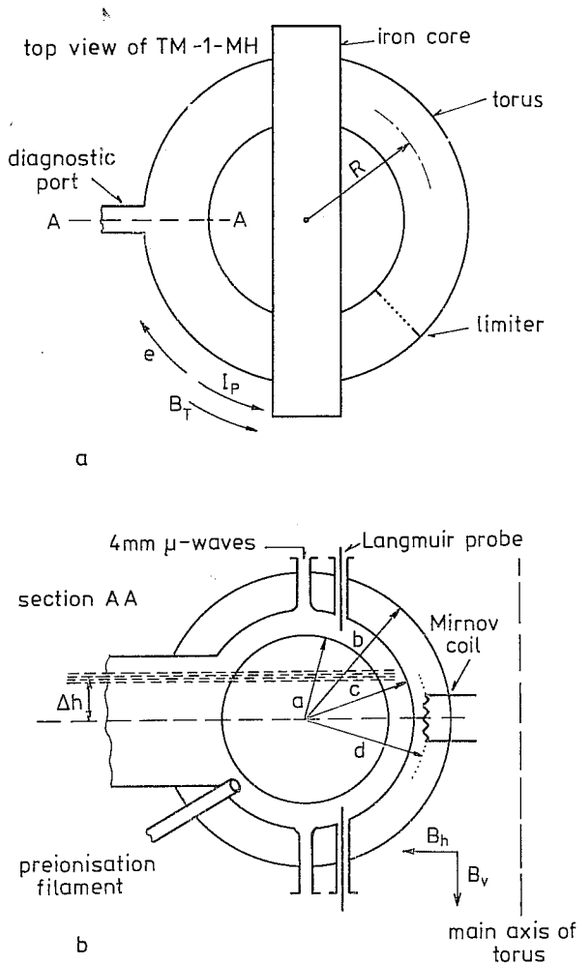

Fig. 1. Geometry of the TM-1-MH breakdown experiment. a) Top view of the torus with the directions of current and magnetic field. b) Diagnostic port (cross-section AA). Limiter and 4 Mirnov coils are not located in this cross-section. Limiter radius $a = 0{\cdot}075$ m; copper shell radius $b = 0{\cdot}135$ m; liner radius $c = 0{\cdot}10$ m; position of Mirnov coils $d = 0{\cdot}115$ m. Arrows indicate the direction of external $B_\perp$ fields.

We made a series of shots with varying B_v and B_h in order to reveal the influence of these fields on the current rise and the temporal evolution of the other plasma parameters.

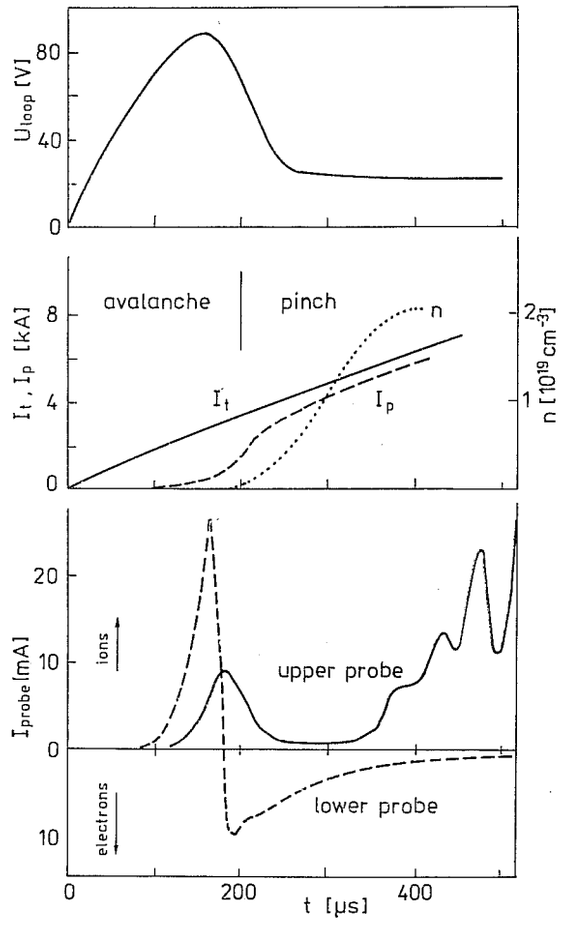

Fig. 2. Temporal evolution of the plasma during the first 500 μs after OH-battery ignition. Top: Loop voltage U_l. Center: Total and plasma current I_t, I_p; electron density from 4 mm μ-wave interferometer. Bottom: Langmuir probe current, both probes are at $r = 80$ mm, $U_p = -60$ V.

The temporal evolution of a typical discharge is shown in fig. 2. The data of loop voltage U_l, total current I_t (liner plus plasma current), mean electron density n (from 4 mm microwave interferometer), and ion saturation current I_+ of the probe in the

limiter shadow can be measured directly. The plasma current I_p is obtained from the total current I_t and the loop voltage U_l:

$$I_p = I_t - I_l = I_t - \frac{U_l}{R_l}.$$

The ohmic liner resistance R_l has been determined from shots without plasma and also from the first 100 μs of a plasma discharge to $R_l = 40$ mOhm. The inductive part of the liner current can be neglected ($L_l < 40$ nH). The Langmuir probe signal showing the density of the scrape off layer (SOL) plasma can be used to distinguish the different regimes of plasma formation. Within the first 150 ... 200 μs (the avalanche phase) the breakdown in the whole cross section of the liner takes place. In the following time period from $t = 200$ μs to $t = 350$ μs (the pinch phase) the plasma disappears from limiter shadow owing to the starting of the confinement. After that the probe signal indicates again the presence of plasma which moves from the center into the limiter shadow forming there the SOL plasma of the stationary state.

Three typical current rises in dependence on the external B_v and B_h fields are shown in fig. 3. The avalanche phase is characterized by an exponential growth $\sim \exp(\gamma t)$ the time constant $1/\gamma$ of which depends on the perpendicular fields. The next period with the slower increase is the pinch phase starting above $I_p \doteq 1$ kA.

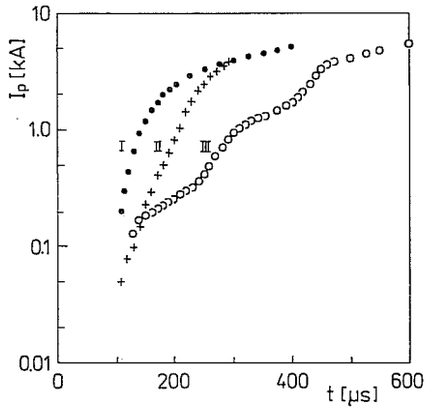

Fig. 3. Temporal evolution of the plasma current for different $B_\perp$-fields. Curve I: $B_v = 5{\cdot}6 \times 10^{-4}$ T, $B_h = 6{\cdot}5 \times 10^{-4}$ T; curve II: $B_v = 16{\cdot}8 \times 10^{-4}$ T, $B_h = 11{\cdot}4 \times 10^{-4}$ T; curve III: $B_v = 22{\cdot}4 \times 10^{-4}$ T, $B_h = 19{\cdot}5 \times 10^{-4}$ T.

A strong change of the radial profile of the plasma column takes place during the process of breakdown and the evolution of the tokamak plasma. The avalanche phase is characterized by a homogeneous distribution with a flat profile. Both probes (upper and lower) show nearly equal values of ion saturation current (fig. 4a). The spatial profile of the H_β-radiation is also flat in that time interval. A clear change starts at the end of the avalanche phase with a peaked plasma profile (fig. 4b). All three diagnostic methods (Langmuir probe, H_β-radiation and Mirnov coils) show the effect that after avalanche phase the plasma column first appears in the lower part of the liner cross section and then moves upwards. The difference in density measured

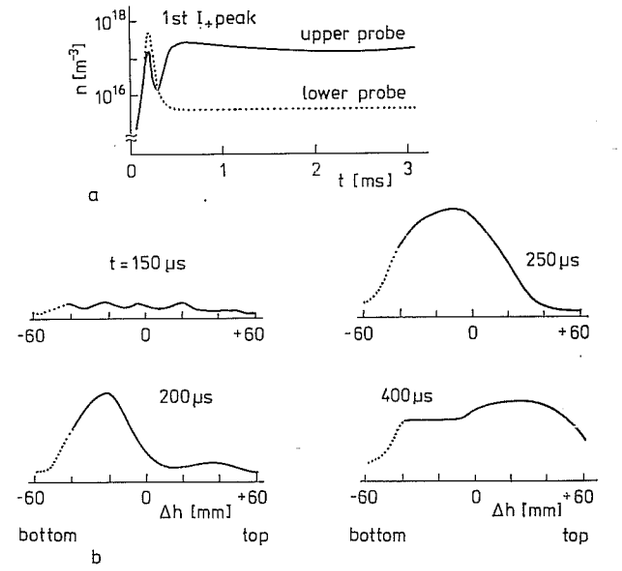

Fig. 4. Temporal evolution of the radial plasma profile. a) SOL-plasma density from ion saturation current. b) H_β line radiance (rel. units). The optical chord is disturbed by the preionization filament for $\Delta h < -50$ mm.

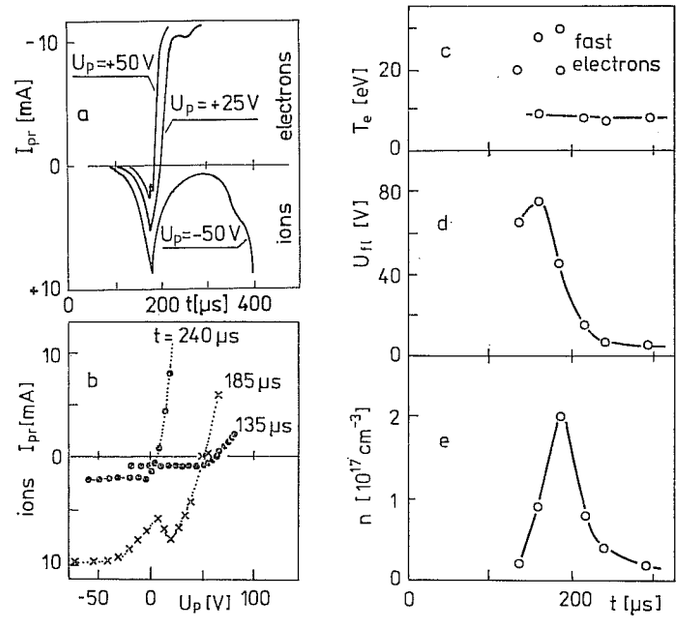

Fig. 5. Langmuir probe measurement in the SOL-plasma, $r = 80$ mm. a) Oscilloscope traces of the probe current for a fixed bias. b) Langmuir probe characteristics taken from a). c) Electron energy kT_e. d) Floating potential U_{fl}. e) Plasma density from ion saturation current.

by the upper and the lower probe is two orders of magnitude. That plasma position is present in every normal shot and cannot be influenced by the external perpendicular fields. An increase of B_h to press the plasma down leads only to disruptive instabilities.

The results of probe measurements in the SOL-plasma are shown in fig. 5. Besides the routine observation of the ion saturation current we made a series of probe current measurements in subsequent shots with a constant bias voltage for every shot. From these curves the Langmuir probe characteristics of fig. 5b were composed. There are indications for fast electrons in the avalanche phase (up to 180 μs) and a bulk electron temperature of 7–10 eV during the first 300 μs (fig. 5c). The floating potential decreases from $U_{fl} = 70 \dots 80$ V to 5 V during the pinch phase (fig. 5d). The density of the wall plasma decreases simultaneously (fig. 5e). No fast electrons are present in this time period.

3. MODEL OF THE AVALANCHE PHASE

A complete theoretical description must include the simultaneous solution of many nonlinear equations. These are: energy and particle balance, Maxwell's equations for the plasma, heat transfer and radiation losses and the equations for the external electrical circuit. An additional difficulty arises if runaway electrons have to be accounted for. To our knowledge the most comprehensive treatment was done in [6].

The present model is much more restricted. It should be a guide to interpreting the experimental facts and to giving an explanation of some physical processes on the basis of the experiments. The most striking facts are the fast current rise in the avalanche phase and its dependence on the auxiliary perpendicular magnetic fields. Consequently the model is limited to these phenomena.

3.1. Temporal growth of the mean electron density

During the start up phase the ionization is determined by the electric field $E_T = U_l/2\pi R$ impressed to the torus by the OH-battery. The temporal growth of the electron density is given by a balance between the ionization rate ν^i and the carrier loss rate β:

$$n \sim \exp \gamma_n t = \exp (\nu^i - \beta)\, t\,. \tag{1}$$

The ionization rate $\nu^i = \alpha(E)\, v_d(E)$ is determined by Townsend's first coefficient $\alpha(E)$ and the electron drift velocity $v_d(E)$. If the value of E/p is not too high, the electrical force eE is balanced by the frictional force of electron neutral collisions resulting in a constant value of v_d. This consideration is based upon the assumption that the electric field E inside the plasma is homogeneously distributed and constant during the avalanche phase. Neither skin effect nor relaxation due to poloidal field build up is important. The electron density is assumed constant over the cross section of the liner. We will show in sec. 3.2 that these assumptions are reasonable.

The loss rate β is determined by the spiral particle trajectories inside the torus. Electrons starting from the center of the vacuum chamber attain the limiter radius after a finite life time t_1 and are lost. They move along helical trajectories resulting from the toroidal and the centrifugal drift and from the helical motion due to external magnetic fields B_v and B_h. Diffusive losses are negligible comparing with this process. We refer to an analysis of the different electron drift orbits in tokamak geometry[13] to calculate the drift losses.

The most important effect for our experimental situation is the helical motion of electrons due to the external perpendicular magnetic fields B_v and B_h. The electrons move antiparallel to the toroidal magnetic field B_T. Together with the usually downward directed B_v field results an upward directed velocity component

$$v_z = -v_d \frac{B_v}{B_T}\,. \tag{2}$$

In a similar way the external horizontal field B_h (usually outward directed) produces an inward drift component:

$$v_x = -v_d \frac{B_h}{B_T}\,. \tag{3}$$

The motion of the guiding center in the poloidal direction is negligible as long as the poloidal magnetic field B_{pol} due to the plasma current is sufficiently small. So the trajectories are straight lines given by eqs. (2) and (3).

The life time of electrons starting near the center of the liner is given by:

$$t_1 = \frac{aB_T}{v_d (B_v^2 + B_h^2)^{1/2}}\,, \tag{4}$$

a = limiter radius. An improved analysis [14] shows the validity of eq. (4) for the conditions:

$$(B_v^2 + B_h^2)^{1/2} \gg \frac{aB_{pol}(r)}{r} \tag{5}$$

or

$$(B_v^2 + B_h^2)^{1/2} \gg 26{\cdot}7 \times 10^{-4} I_p\ (\mathrm{T, kA})\,.$$

The growth rate of the electron density γ_n follows from the substitution of eq. (4) with $t_1 = \beta^{-1}$ into eq. (1)

$$\gamma_n = \nu^i(E) \left\{ 1 - \frac{(B_v^2 + B_h^2)^{1/2}}{\alpha(E)\,.\,a\,.\,B_T} \right\}. \tag{6}$$

This formula predicts a clear dependence of γ_n on the external magnetic fields which should be observable in the experiment. On the other hand it predicts a threshold for the electric field by the condition $\gamma_n = 0$ for a given combination of the magnetic field.

3.2. Evolution of plasma field and current

The ionization frequency ν^i and the Townsend coeficient α depend on the electric field strength E. This field inside the plasma can be smaller than the externally impressed toroidal field E_T. For a comparison of eq. (6) with the experiment the electron density $n(t)$ must be known. We do not have the possibility of measuring actual values of both quantities. The plasma electric field E cannot be measured and the electron density $n < 10^{18}\,\mathrm{m}^{-3}$ during the avalanche phase is too low for the 4 mm microwave interferometer. Therefore we must utilize the ohmic resistance of the plasma loop obtained from measurements of the loop voltage and plasma current. Such an approach requires the discussion of the following problems: a) The temporal variation of the plasma conductivity $\sigma(t)$ caused by the change of the electron density. b) The relaxation of the plasma electric field and current density when the poloidal magnetic field is built up. c) The feedback of E upon ionization and loss processes, i.e. on the growth rate γ_n. d) The prevention of field penetration caused by a fast change of the conductivity (skin effect).

Let us first show that c) and d) need not be considered in detail for the present experimental conditions, a fact substantially simplifying the problem. The applied field E_T is well above the threshold and varies only weakly. For a change of E, say $\pm 50\%$ during the avalanche phase, we can neglect this influence on $\gamma_n (\gamma_n \sim E^{1/2})$. Therefore the electron density n and the conductivity σ are purely time depending (parametric) quantities.

The skin effect can be estimated as a diffusion of the current density $J(r, t)$. We derive a diffusion equation from Maxwell's equations with $(\mu_0\,\sigma(t))^{-1}$ as an equivalent diffusion coefficient. A disturbance at the plasma boundary propagates radially towards the axis within a time given by

$$t_{\mathrm{diff}} \simeq \frac{a^2}{2D_{\mathrm{eq}}} = \tfrac{1}{2} a^2 \mu_0\,\sigma(t)\,. \tag{7}$$

The radial distribution of the current density remains homogeneous as long as $J \Big/ \left(\frac{\partial J}{\partial t}\right)_{r=a} > t_{\mathrm{diff}}$, i.e. sufficiently slow processes. For an estimation we substitute $J \Big/ \left(\frac{\partial J}{\partial t}\right)_{r=a} \simeq I_p \left(\frac{\mathrm{d}I_p}{\partial t}\right)$ and neglect the skin effect whenever the condition

$$t_{\mathrm{diff}} \lesssim I_p \Big/ \left(\frac{\mathrm{d}I_p}{\mathrm{d}t}\right) \tag{8}$$

is fulfilled [14].

The discussion a) and b) starts with the plasma current given by

$$I_p(t) = \int 2\pi r\, J(r, t)\,\mathrm{d}r \simeq \pi a^2\, J(t) \tag{9}$$

and the ohmic plasma resistance per unit of length

$$R' = 1/(a^2\pi\,\sigma(t))\,. \tag{10}$$

The plasma current evolves from the relaxation equation

$$L' \frac{\mathrm{d}I_p(t)}{\mathrm{d}t} + R'(t)\, I_p(t) = E_T(t)\,. \tag{11}$$

Here L' is the inductance of the plasma loop[1]) and $E_T(t)$ the externally impressed toroidal field strength. With the initial condition $I_p\,(t = 0) = 0$ the solution of eq. (11) can be written as:

$$I_p(t) = \exp\left[-\int_0^t \frac{\mathrm{d}t'}{\tau(t')}\right] \cdot \int_0^t \frac{E_T(t'')}{L'} \exp\left[\int_0^{t''} \frac{\mathrm{d}t'}{\tau(t')}\right] \mathrm{d}t'' \tag{12}$$

with $\tau = a^2\pi\,\sigma(t)\,L'$.

In order to apply eq. (12) the conductivity $\sigma(t)$ must be specified. During the main part of the avalanche phase the plasma is weakly ionized and its conductivity is determined by electron-hydrogen collisions. The drift velocity of electrons is proportional to $E^{1/2}$ (eq. (18)) at high values of E/p. Accounting for the decreasing number of neutral particles during the ionization process we obtain:

$$\sigma_{e0} = 1{\cdot}8 \times 10^{-4} \frac{n}{(n_H - n)\,(E/n_H)^{1/2}}\,; \quad (\Omega^{-1}\mathrm{m}^{-1}, \mathrm{m}^{-3}, \mathrm{V/m})\,. \tag{13}$$

The coulomb term of the conductivity is given by

$$\sigma_{ei} = 1{\cdot}9 \times 10^{4} \frac{T_e^{3/2}}{Z \ln \Lambda}\,; \quad (\Omega^{-1}\mathrm{m}^{-1}, \mathrm{eV})\,, \tag{14}$$

where $\ln \Lambda$ is the coulomb logarithm and $Z = 1$ for hydrogen. The total conductivity follows from

$$\sigma^{-1} = \sigma_{e0}^{-1} + \sigma_{ei}^{-1}\,. \tag{15}$$

At the beginning of the avalanche phase we have $n \ll n_H$ and $\sigma = \sigma_{e0} \sim n \sim$ $\sim \exp(\gamma_n t)$. At the end of this phase the degree of ionization is high and the coulomb conductivity which is independent of electron density is reached. A simple formula

[1]) The inductance per unit length is given by

$$L' = \frac{\mu_0}{2\pi}\left[\ln\frac{b}{a} + \frac{\int B_{\mathrm{pol}}^2 r\,\mathrm{d}r}{a^2\, B_{\mathrm{pol}}^2(a)}\right],$$

$b =$ radius for $B_{\mathrm{pol}} = 0$ (approx. radius of copper shell). During the avalanche phase the current distribution can be assumed homogeneous and the second term in parenthesis becomes 1/4. So we obtain $L' \simeq 2 \times 10^{-7}$ H/m.

which reproduces these facts is given by

$$\sigma(t) = \frac{\sigma_0 \sigma_{ei} \exp(\gamma_n t)}{\sigma_{ei} + \sigma_0 \exp(\gamma_n t)}, \tag{16}$$

where σ_0 is the conductivity at the very beginning[2]).

We have enumerated the plasma current for a step function of the electric field: $E_T = 0$ at $t < 0$; $E_T = 20$ V/m at $t > 0$, $\sigma_0 = 1\,\Omega^{-1}\mathrm{m}^{-1}$, $\sigma_{ei} = 5 \times 10^4\,\Omega^{-1}\mathrm{m}^{-1}$ and $\gamma_n = 3 \times 10^4\,\mathrm{s}^{-1}$. The initial conductivity corresponds to an electron density $n = 10^{14}\,\mathrm{m}^{-3}$ and σ_{ei} to a temperature $T_e = 10$ eV (see eq. (14)). The other parameters are $R = 0{\cdot}4$ m, $a = 0{\cdot}075$ m and $L' = 2 \times 10^{-7}$ H/m.

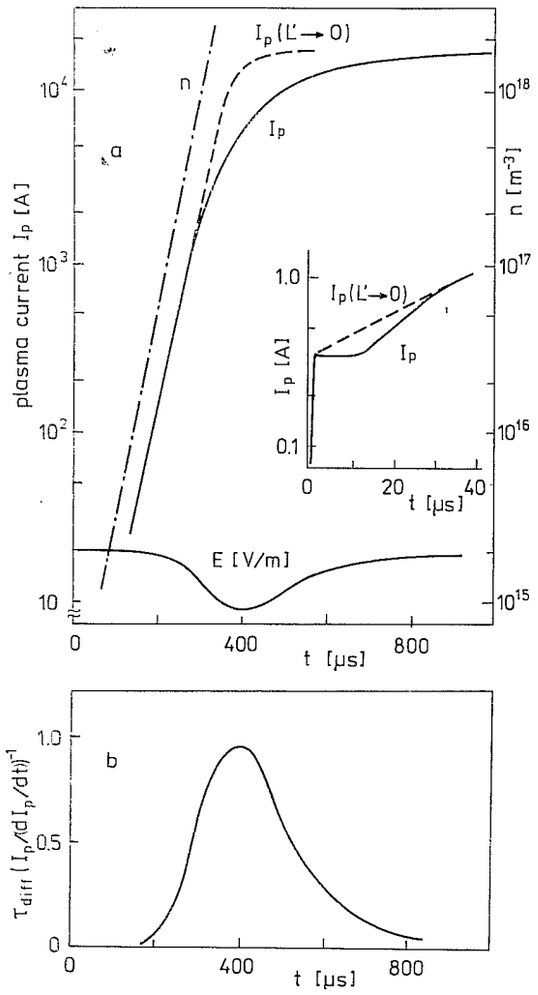

Fig. 6. Results of skin effect estimation. a) Evolution of plasma current I_p and electric field E after a step of the loop voltage at $t = 0$. Inset: Delay of current growth in the first 40 μs. b) Ratio of field diffusion time t_{diff} to the time scale of plasma current characterizing the skin effect.

[2]) σ_0 corresponds to an initial electron density $n \simeq 10^{13} \ldots 10^{14}$ m^{-3} produced by the preionization source.

The result of the numerical calculation is shown in fig. 6a together with the value $I_p(t)$ for $L' \to 0$. At the very beginning ($t \lesssim 20$ μs) the plasma current shows a delay compared with the curve for $L' \to 0$. Another delay is obtained before the current reaches its stationary value. In the meantime the current grows at the same rate as the conductivity. The ohmic component of the plasma field E and the electron density are also shown in fig. 6a. The relation $t_{\mathrm{diff}} \Big/ \left(\frac{I_p}{\mathrm{d}I_p/\mathrm{d}t}\right)$ is plotted in fig. 6b. The results show clearly that only in the time interval 320–460 μs the skin effect is expected to be significant. It can be neglected during the major part of the avalanche phase. Therefore the growth rate of the electron density γ_n within the first 300 μs can be obtained from the plasma current.

4. COMPARISON WITH THE EXPERIMENT

A logarithmic plot of the plasma current for the three typical shots with different values of the external perpendicular field B_T is shown in fig. 3. Two shots show an exponential increase at the beginning with $\gamma = 3 \div 5 \times 10^4\,\mathrm{s}^{-1}$, the third is more complicated. If we disregard the periodic structure of this curve we obtain $\gamma \simeq$ $\simeq 10^4\,\mathrm{s}^{-1}$. From these curves and the associated values of the loop voltage the ohmic plasma resistance

$$R'(t) = \frac{1}{I_p}\left[E_T(t) - L'(\mathrm{d}I_p/\mathrm{d}t)\right] \tag{17}$$

and the corresponding mean values of conductivity and electron density were calculated. The electron density $n(t)$ grows exponentially with a time constant γ_n^{-1} as expected. The values are given in tab. 1 together with the extrapolated initial density ($t \to 0$). The calculations were done with $n_H = 10^{19}\,\mathrm{m}^{-3}$, $Z = 1$, $T_e = 10$ eV and the actual value of E which was between 12 and 36 V/m.

Table 1

Current of external	I_h(A)	100	175	300
field coil	I_v(A)	200	600	800
γ	(s^{-1})	4×10^4	$3{\cdot}3 \times 10^4$	10^4
$n(t = 0)$	(m^{-3})	5×10^{14}	3×10^{14}	6×10^{15}

The determination of the ionization parameters ν^i and α from eq. (6) requires the knowledge of the magnetic field inside the plasma. It is a combination of several components, only some of them can be calculated or measured exactly [15]:

1. The deliberately applied fields B_v^{ext} and B_h^{ext} generated by external currents parallel to the plasma axis which control the plasma position.

which reproduces these facts is given by

$$\sigma(t) = \frac{\sigma_0 \sigma_{ei} \exp(\gamma_n t)}{\sigma_{ei} + \sigma_0 \exp(\gamma_n t)}, \tag{16}$$

where σ_0 is the conductivity at the very beginning[2]).

We have enumerated the plasma current for a step function of the electric field: $E_T = 0$ at $t < 0$; $E_T = 20$ V/m at $t > 0$, $\sigma_0 = 1\,\Omega^{-1}\mathrm{m}^{-1}$, $\sigma_{ei} = 5 \times 10^4\,\Omega^{-1}\mathrm{m}^{-1}$ and $\gamma_n = 3 \times 10^4\,\mathrm{s}^{-1}$. The initial conductivity corresponds to an electron density $n = 10^{14}\,\mathrm{m}^{-3}$ and σ_{ei} to a temperature $T_e = 10$ eV (see eq. (14)). The other parameters are $R = 0{\cdot}4$ m, $a = 0{\cdot}075$ m and $L' = 2 \times 10^{-7}$ H/m.

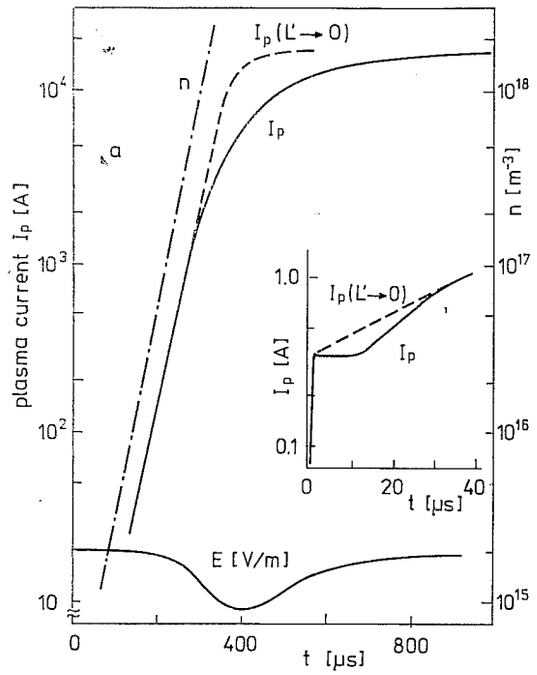

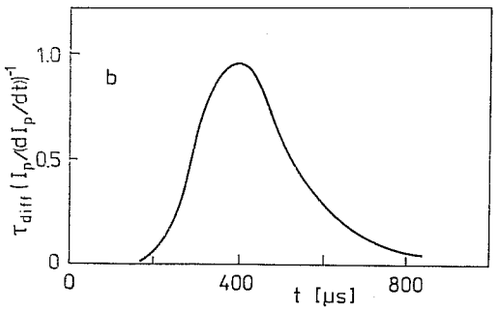

Fig. 6. Results of skin effect estimation. a) Evolution of plasma current I_p and electric field E after a step of the loop voltage at $t = 0$. Inset: Delay of current growth in the first 40 μs. b) Ratio of field diffusion time t_{diff} to the time scale of plasma current characterizing the skin effect.

[2]) σ_0 corresponds to an initial electron density $n \simeq 10^{13} \ldots 10^{14}$ m^{-3} produced by the preionization source.

The result of the numerical calculation is shown in fig. 6a together with the value $I_p(t)$ for $L' \to 0$. At the very beginning ($t \lesssim 20$ μs) the plasma current shows a delay compared with the curve for $L' \to 0$. Another delay is obtained before the current reaches its stationary value. In the meantime the current grows at the same rate as the conductivity. The ohmic component of the plasma field E and the electron density are also shown in fig. 6a. The relation $t_{\mathrm{diff}} \Big/ \left(\frac{I_p}{\mathrm{d}I_p/\mathrm{d}t}\right)$ is plotted in fig. 6b. The results show clearly that only in the time interval 320–460 μs the skin effect is expected to be significant. It can be neglected during the major part of the avalanche phase. Therefore the growth rate of the electron density γ_n within the first 300 μs can be obtained from the plasma current.

4. COMPARISON WITH THE EXPERIMENT

A logarithmic plot of the plasma current for the three typical shots with different values of the external perpendicular field B_T is shown in fig. 3. Two shots show an exponential increase at the beginning with $\gamma = 3 \div 5 \times 10^4\,\mathrm{s}^{-1}$, the third is more complicated. If we disregard the periodic structure of this curve we obtain $\gamma \simeq$ $\simeq 10^4\,\mathrm{s}^{-1}$. From these curves and the associated values of the loop voltage the ohmic plasma resistance

$$R'(t) = \frac{1}{I_p}\left[E_T(t) - L'(\mathrm{d}I_p/\mathrm{d}t)\right] \tag{17}$$

and the corresponding mean values of conductivity and electron density were calculated. The electron density $n(t)$ grows exponentially with a time constant γ_n^{-1} as expected. The values are given in tab. 1 together with the extrapolated initial density ($t \to 0$). The calculations were done with $n_H = 10^{19}\,\mathrm{m}^{-3}$, $Z = 1$, $T_e = 10$ eV and the actual value of E which was between 12 and 36 V/m.

Table 1

Current of external	I_h(A)	100	175	300
field coil	I_v(A)	200	600	800
γ	(s^{-1})	4×10^4	$3{\cdot}3 \times 10^4$	10^4
$n(t=0)$	(m^{-3})	5×10^{14}	3×10^{14}	6×10^{15}

The determination of the ionization parameters ν^i and α from eq. (6) requires the knowledge of the magnetic field inside the plasma. It is a combination of several components, only some of them can be calculated or measured exactly [15]:

1. The deliberately applied fields B_v^{ext} and B_h^{ext} generated by external currents parallel to the plasma axis which control the plasma position.

2. Perpendicular fields caused by the inhomogeneous distribution of the current in the liner and by eddy currents in the copper shell.
3. $B_\perp$-components from the misalignment of the toroidal field coils.
4. Stray fields from the iron transformer core.

The contributions 2, 3, 4 can hardly be calculated but they play a role at the beginning of the start up phase when the liner current is bigger than the plasma current. We tried to measure these fields by means of Mirnov-coils. The result was $B_v^{\text{int}} = -8{\cdot}4 \times \times 10^{-4}$, $B_h^{\text{int}} \doteq -11{\cdot}4 \times 10^{-4}$ T in the opposite direction to the external fields acc. to point (1). The procedure has been described in [14]. Mainly two restraints, however, limit the reliability of this method: a) The internal fields are determined at the position of the Mirnov-coils; it is doubtful whether they are constant along the

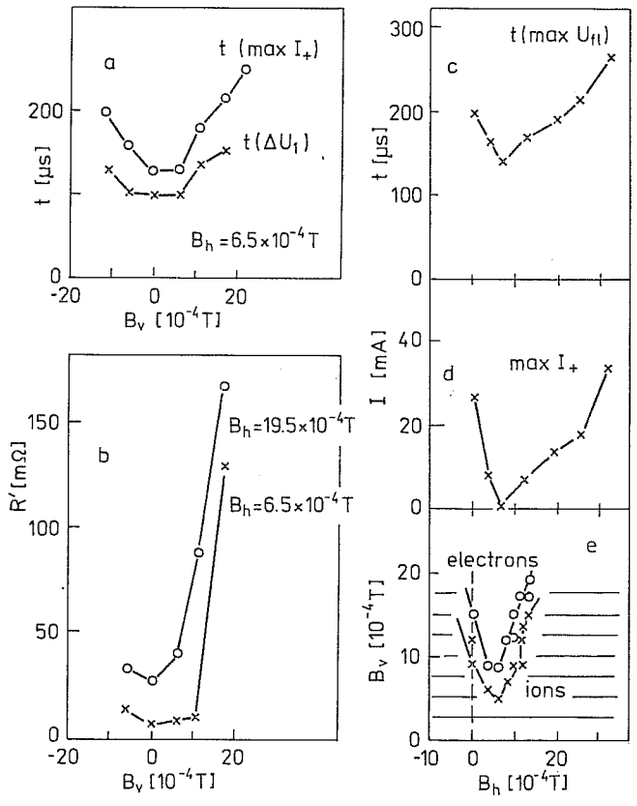

Fig. 7. Estimation of the actual internal $B_\perp$-field. Variation of B_v (external coil) a, b; variation of B_h (external coil) c, d. a) Time of first maximum I_+ (cf. fig. 4a); time of deviation of the loop voltage with plasma from that without plasma. b) Ohmic plasma resistance at $t = 200$ μs. c) Time of the maximum U_{fl} in the SOL-plasma. d) Maximum value of ion saturation current I_+ (upper probe). e) Change of direction of upper probe current (from ions to electrons) in dependence on both external magnetic fields. No bias, probe connected via 80 Ω to liner.

circumference of the torus. b) Measurements are possible only at times with sufficiently big plasma current ($t > 300$ μs) when the avalanche phase has already finished. These uncertainties induced us to look for some additional hints for the actual magnitude of the perpendicular fields $B_\perp = B^{\text{ext}} + B^{\text{int}}$ during the avalanche phase. We measured the $B_\perp$-dependence of some quantities related to breakdown (fig. 7). The minima of all these curves are shifted by $B_v \simeq 3 \times 10^{-4}$ T and $B_h \simeq \simeq 6{\cdot}5 \times 10^{-4}$ T with respect to the zero $B_\perp$-field. On condition that breakdown is optimal for $B_\perp = 0$, we conclude that the internal fields equal these smaller values. The internal fields of the T7 Tokamak [9] and that of the JFT-2 instalation [7] determined by a similar procedure were found to be in the same range.

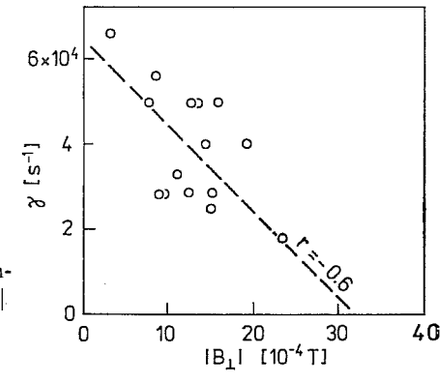

Fig. 8. Measured current growth rate γ in dependence on the total perpendicular magnetic field $|B_\perp|$

The measured values of γ_n versus the internal magnetic field $|B_\perp| = [(B_h^{\text{ext}} - 6{\cdot}5 \times \times 10^{-4}\,\text{T})^2 + (B_v^{\text{ext}} - 3 \times 10^{-4}\,\text{T})^2]^{1/2}$ are shown in fig. 8. The experimental points agree fairly well with a straight line (correlation coefficient $r = -0{\cdot}6$) corresponding to eq. (6). We obtain $\gamma_n(B = 0) \simeq \nu^i = 6{\cdot}5 \times 10^4\,\text{s}^{-1}$ and the first Townsend coefficient $\alpha = 3{\cdot}3 \times 10^{-2}\,\text{m}^{-1}$. From α and ν^i it follows for the electron drift velocity that $v_d = 2 \times 10^6$ m/s.

5. DISCUSSION AND CONCLUSIONS

The present experiments were carried out in hydrogen gas with a constant filling pressure of $p = 1{\cdot}3 \times 10^{-2}$ Pa (10^{-4} Torr). Let us assume that during the start up phase of the tokamak discharge the gas influx from the chamber wall does not yet take place and the avalanche electrons collide with hydrogen molecules only. Then our experimental value $\alpha/p = 2{\cdot}5\,\text{m}^{-1}\,\text{Pa}^{-1}$ can be compared with the well-known values of the Townsend coefficient for high values of $E/p = 7 \times 10^2 - 2 \times 10^3$ V/mPa. At these high values, in particular if the pressure is low, a significant part of the electrons can run away. Experimental and theoretical investigations of the drift velocity in hydrogen at high values of E/p are shown in fig. 9 [11, 12]. The experimental points are well approximated by the lower branch of the theoretical curve [11] in the range $10^2 < E/p < 5 \times 10^2$ V/mPa. For higher values of E/p the electron

distribution function becomes strongly non-Maxwellian. In a recent paper this problem has been treated for a high temperature plasma [16]. Usually, for $E/p > 5 \times 10^2$ V/mPa the theory predicts runaway electrons. The experiments [12], however, show that up to $E/p = 1{\cdot}5 \times 10^3$ V/mPa the drift model seems to be still valid. Therefore the approximation

$$v_d = 6{\cdot}9 \times 10^4 \left(\frac{E}{p}\right)^{1/2}; \quad \text{(m/s, V/m, Pa)} \tag{18}$$

can be used within the range of $70 \leqq E/p \leqq 1{\cdot}5 \times 10^3$ V/mPa. The extrapolation from small E/p-values leads to the approximation $v_d = 4{\cdot}7 \times 10^3\, E/p$ [4].

Similar discrepancies exist for the first Townsend coefficient. The values α/p given by various authors are plotted in fig. 10. At high values of E/p a significant part of the electrons is in a runaway state and does not contribute to ionization. Measurements at low pressure back the supposition that especially with decreasing gas density this effect becomes more and more important [17]. A detailed theoretical paper [11] also shows the effect of decreasing ionization with increasing E/p. Only the upper and lower limits of α/p from [11] are shown in fig. 10 since the effect is sensitive to several parameters. Our experimental results are in accordance with this interpretation.

The following conclusions can be drawn:

1. The time delay between the start of the OH-battery and the first signal of plasma current and density is determined by the exponential growth of an electron avalanche starting from the density given by the preionization source.

2. The carrier production is controlled by the electron drift velocity in the toroidal electric field.

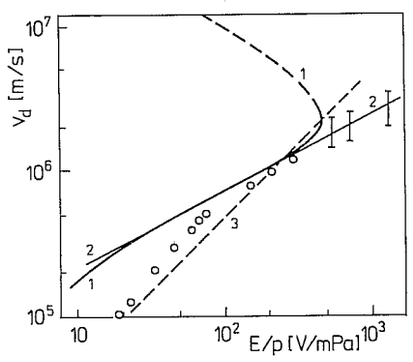

Fig. 9. Electron drift velocity in hydrogen. Experimental values [12] ∘∘∘ III. Curve 1: calculated for moderate runaway regime [11]; curve 2: approximation eq. (18); curve 3: approximation [4].

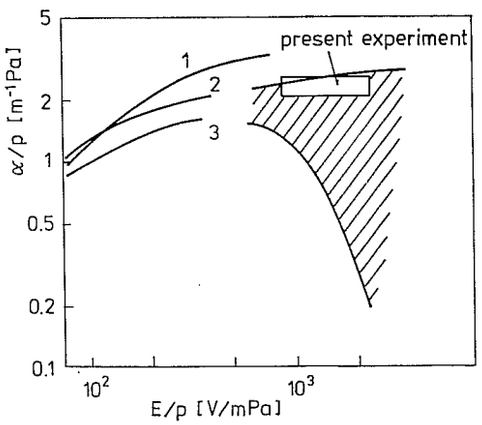

Fig. 10. Ionization coefficient in hydrogen [11]. Curves 1, 2, 3: experimental values from gas discharge physics. Hatched area: modification by runaway electrons. □: results of present experiment.

3. After the exponential phase a pinch occurs where the plasma loses the wall contact, the temperature increases up to ~10 eV and the ionization becomes thermal. Current density and electron density grow much more slowly than in the avalanche state. The conductivity is determined mainly by the coulomb collisions.

4. The time constant of the exponential growth is given by a balance of ionization and carrier losses. These losses are determined by the auxiliary perpendicular magnetic fields which control the different drift motions of the electrons in the avalanche state. The smallest losses, i.e. the fastest current rise, occur for vanishing perpendicular fields.

5. The skin effect and the relaxation of poloidal field growth are not important during the avalanche phase since the conditions $I_p \Big/ \left(\frac{dI_p}{dt}\right) \gg t_{\text{diff}}, \tau$ are fulfilled. Therefore current density, Ohmic and inductive parts of the plasma impedance and the electric field inside the plasma can be obtained from measurements of loop voltage and plasma current only. These values fit in the results obtained by the usual diagnostics, e.g. microwave interferometry in the later states.

6. The value of the first Townsend coefficient $\alpha/p = 2{\cdot}5\ \text{m}^{-1}\text{Pa}^{-1}$ at $E/p = 1{\cdot}5 \times 10^3$ V/mPa is smaller than that known from gas discharge physics. It can be explained by a moderate runaway regime. This runaway regime does not outlive the start up phase since the main tokamak discharge in quite normal.

Two of us (H.P. and P.H.) wish to thank the TM-1-MH team for cooperation during the experiments and operation of the machine.

Received 18. 11. 1983.

References

[1] Dimock D. L. et al.: Nucl. Fusion *13* (1973) 271.
[2] Hutchinson I. H., Strachan J. D.: Nucl. Fusion *14* (1974) 649.
[3] Strachan J. D.: Nucl. Fusion *16* (1976) 345.
[4] Papoular R.: Nucl. Fusion *16* (1976) 37.
[5] Abramov V. A. et al.: Fiz. Plazmy *1* (1975) 536.
[6] Abramov V. A. et al.: Fiz. Plazmy *3* (1977) 512.
[7] Sometani T., Fujisawa N.: Plasma Physics *20* (1978) 1101.
[8] Strachan J. D.: Nucl. Mater. *63* (1976) 132.
[9] Denisov V. F. et al.: Fiz. Plazmy *8* (1982) 238.
[10] Ďatlov J. et al.: *in* Proc. IX. European Conf. on Controlled Fusion and Plasma Physis, Vol. 1, Oxford 1979, p. 539.
[11] Müller K. G.: Z. Phys. *169* (1962) 432.
[12] Schlumbohm H.: Z. Phys. *182* (1965) 317.
[13] Knoepfel H., Spong D. A.: Nucl. Fusion *19* (1979) 785.
[14] Prinzler H. et al.: ZIE Preprint 83 — 3, May 1983.
[15] Mukhovatov V. S., Shafranov V. D.: Nucl. Fusion *11* (1971) 605.
[16] Kusnetsov Yu. K., Lebed S. A.: Fiz. Plazmy *8* (1982) 1269.
[17] Buffa A. et al.: Phys. Rev. A*3* (1971) 955.